Current Applied Physics 20 (2020) 320–325

Contents lists available at ScienceDirect

Current Applied Physics

journal homepage: www.elsevier.com/locate/cap

Magnetic iron oxide nanoparticle-hollow mesoporous silica Spheres:Fabrication and potential application in drug delivery

Yun Teng[a], Yimeng Du[a], Jue Shi[b], Philip W.T. Pong[a,*]

[a] Department of Electrical and Electronic Engineering, The University of Hong Kong, Hong Kong
[b] Department of Physics, Hong Kong Baptist University, Hong Kong

ARTICLE INFO

Keywords:
Magnetic nanoparticles
Mesoporous silica spheres
Adsorption capacity and loading efficiency
pH-triggred release
Cell viability

ABSTRACT

A facile method is developed for the fabrication of magnetic iron oxide nanoparticle-hollow mesoporous silica spheres (IONP-HMSs) and explored their potential application in drug delivery. Through the self-assembling process of IONPs and the formation of mesoporous silica shells, the IONP-HMSs with hollow interior cavity were obtained. The cetyltrimethyl ammonium bromide (CTAB) encapsulated IONP-containing spheres served as the template to establish the mesoporous silica shells. Typical anti-cancer drug, doxorubicin hydrochloride (DOX) was applied for drug loading and release process of IONP-HMSs, which demonstrated the IONP-HMSs have a high drug loading efficiency and allow pH-trigged release of DOX *in vitro*. Moreover, the IONP-HMSs exhibited excellent biocompatibility and enhanced DOX therapeutic efficacy to HeLa cells. Compared with traditional methods, the reported microemulsion-based method for the synthesis of IONP-HMSs enables the formation of hollow-structured nanocomposite without any complex template-removing process, which could pave the way to improving the therapeutic efficacy in drug delivery system.

1. Introduction

With the development of drug delivery system, nanostructured functional materials have attracted increasing attention due to the potential to realize high-efficiency cancer therapy [1] by utilizing their unique advantages such as controllable size [2], biocompatibility [3] and reduced side effects [4]. Various kinds of nanoparticles (NPs) such as ceramic NPs [5], liposome [6] and Au NPs [7] have been used as drug nanocarriers. Among them, iron oxide magnetic nanoparticles (IONPs) have attracted extensive interest because of its biocompatibility [8] and magnetic properties [9] for selective targeting [10] and contrast enhancement in magnetic resonance imaging [11]. However, the IONPs lack homogeneous anchoring sites on the surface to interact with other biochemical molecules during the drug delivery process in the biological environment [12]. Mesoporous silica materials can be applied to overcome this problem because their large functionalizable surface and large pore volumes provide them strong affinity to various biomolecules, which is highly conducive to drug delivery application [13–15]. Lin's group has reported that HMSs with an average particle size as big as 600 nm has taken up by cancer and non-cancer cells and could lead to the future development of nanoprobe for intracellular sensing and gene/drug delivery [16]. Consequently, it is of great interest to combine mesoporous silica and IONPs as a promising alternative to developing the potential drug nanocarrier.

Recently, considerable efforts have been devoted to the construction of hollow mesoporous silica to enhance the drug loading efficiency [17]. The hollow mesoporous silica spheres (HMSs) were prepared via the soft/hard-templating routes by removing the interior soft/hard templates to produce the hollow structure of nanocomposite [18]. However, the existing manufacture techniques suffer the issues including complicated experimental set-up and time-consuming process owing to the complexity of removing template [19]. Therefore, the development of a facile approach for hollow mesoporous silica-based nanocomposite is of great significance.

In this work, the magnetic iron oxide nanoparticle-hollow mesoporous silica spheres (IONP-HMSs) were prepared via an oil-in-water microemulsion method, and spheres containing CTAB encapsulated IONP served as the template for the formation of mesoporous silica shells. The demonstrated method of IONP-HMSs could directly be applied for the formation of hollow-structured nanocomposite without any template-removing procedure. Here, the IONP-HMSs served as the nanocarrier and applied in loading and release of doxorubicin hydrochloride (DOX) *in vitro*. Moreover, the cellular cytotoxicity tests were conducted to study the biocompatibility of IONP-HMSs. The efficacy of DOX-loaded IONP-HMSs for cancer therapy was analyzed and discussed.

* Corresponding author.
E-mail addresses: yunteng@eee.hku.hk (Y. Teng), ymdu@eee.hku.hk (Y. Du), jshi@hkbu.edu.hk (J. Shi), ppong@eee.hku.hk (P.W.T. Pong).

https://doi.org/10.1016/j.cap.2019.11.012
Received 5 January 2019; Received in revised form 15 October 2019; Accepted 15 November 2019
Available online 04 December 2019

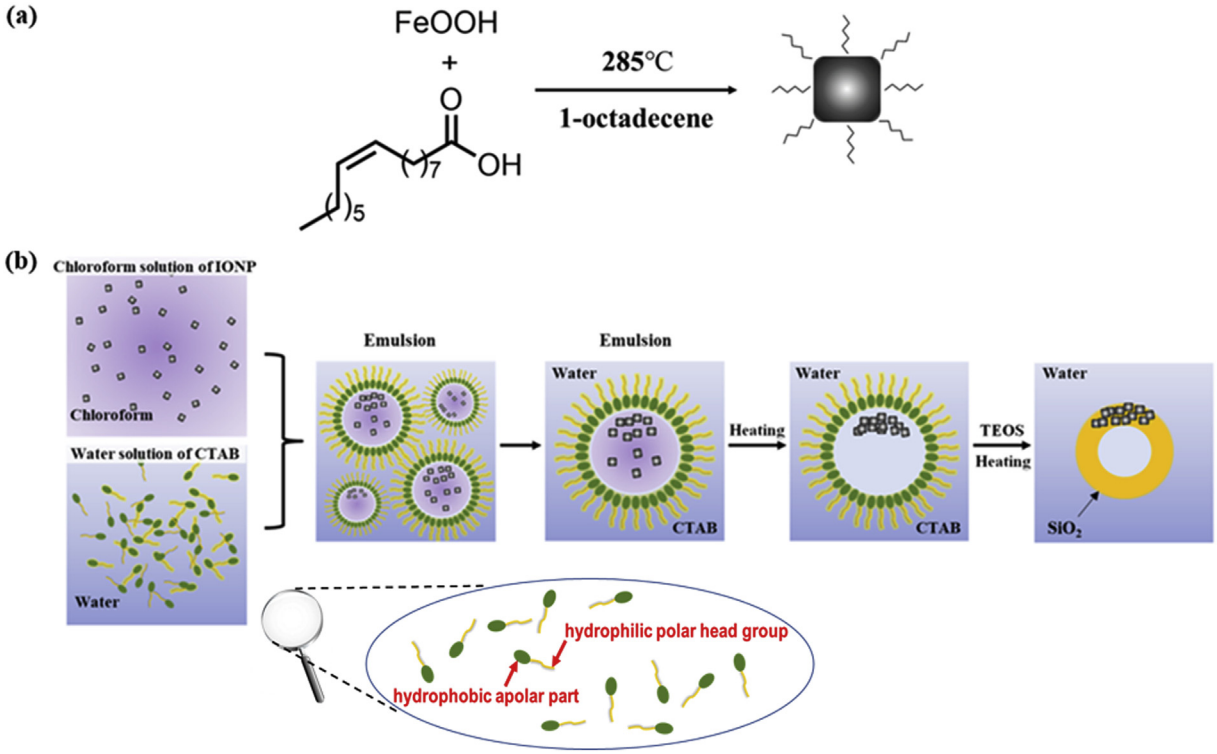

Fig. 1. Schematic illustration of (a) synthesis process of square-shape IONP, and (b) the fabrication procedures of IONP-HMSs.

2. Materials and methods

The IONP-hollow mesoporous silica spheres (IONP-HMSs) were synthesized through an oil-in-water microemulsion method [18]. Firstly, the square-shape IONPs were prepared using the continuous thermal decomposition method [20], as shown in Fig. 1(a). Subsequently, the resulting IONPs were dispersed in chloroform, mixed with the aqueous CTAB solution and incubated in 80 ˚C water bath to evaporate the chloroform. The CTAB encapsulated IONP-containing spheres were formed as templates to direct the formation of hollow mesoporous silica after evaporation. TEOS was added into the solution, and after heating at 95 ˚C for 2 h, a layer of mesoporous silica shell was coated by CTAB encapsulated IONP-containing spheres. Finally, these obtained IONP-HMSs were dried under vacuum for further use.

The drug loading and release process of IONP-HMSs were studied with doxorubicin hydrochloride (DOX). For DOX loading experiment, IONP-HMSs solutions (2 mg/mL) in PBS buffer was mixed with various concentrations of DOX solutions (0–0.9 mg/mL, PBS) and stirred vigorously for 24 h. Unloaded DOX was quantified by measuring the ultraviolet–visible (UV–Vis) absorbance at 480 nm.

The adsorption capacity (wt %) and loading efficiency (%) of the nanocomposite were calculated based on Equation (1) and Equation (2), respectively [21,22].

The drug adsorption capacity (wt %) was calculated according to the following equation:

$$\text{Adsorption Capacity (wt \%)} = \frac{[C_{initial\ DOX} - C_{unbound\ DOX}] * V}{M} * 100 \quad (1)$$

where, $C_{initial\ DOX}$ is the initial DOX concentration, $C_{unbound\ DOX}$ is the concentration of unbound DOX after adsorption. $C_{initial\ DOX}$ and $C_{unbound\ DOX}$ were calculated by measuring DOX concentrations at 480 nm of absorption spectra after calibration. V is the volume of DOX solution and M is the mass of the adsorbent.

The drug loading efficiency (%) was defined as the following equation:

$$\text{Loading Efficiency (\%)} = \frac{C_{initial\ DOX} - C_{unbound\ DOX}}{C_{initial\ DOX}} * 100 \quad (2)$$

where, $C_{initial\ DOX}$ is the initial DOX concentration, $C_{unbound\ DOX}$ is the concentration of unbound DOX after adsorption, which were calculated by measuring DOX concentrations at 480 nm of absorption spectra after calibration.

To estimate the drug release behavior *in vitro*, 3 mL of DOX-loaded IONP-HMSs solution (2 mg/mL, PBS) with pH 5.0 and pH 7.4 were incubated at 37 ˚C, and samples were taken at the different time point. The sample solutions were centrifuged to remove the IONP-HMSs, and the supernatant was collected to measure the released DOX. The released DOX was quantified by measuring the UV–Vis absorbance at 480 nm.

HeLa cells were cultured in DMEM supplemented with 10% (v/v) fetal bovine serum (FBS), penicillin (50 U/mL, Invitrogen), and streptomycin (50 μl/mL, Invitrogen). Cells were incubated at 37 ˚C in a humidified atmosphere with 5% CO_2. The cytotoxicity of DOX-loaded IONP-HMSs was investigated by standard methyl thiazolyl tetrazolium (MTT) assay. The HeLa cells were seeded into 96-well plates and grown overnight. The cells were then incubated with various concentrations of DOX-loaded IONP-HMSs and free DOX for 24 h. After that, the cells were washed with PBS and processed with the standard MTT assay to determine the cell viabilities relative to the untreated cells as control. Briefly, the fresh medium containing MTT reagent with concentration of 0.5 mg/mL was added to each well and incubated for 2 h. After removing the medium, 100 μL of the DMSO was added into the microplate well to dissolve the formazan crystals. The absorbance at 490 nm was recorded for each well of the microplate to determine the cell viability.

3. Results and discussion

The schematic illustration in Fig. 1(b) presents the synthesis procedures of magnetic iron oxide nanoparticle-hollow mesoporous silica spheres (IONP-HMSs). The monodisperse IONPs prepared through

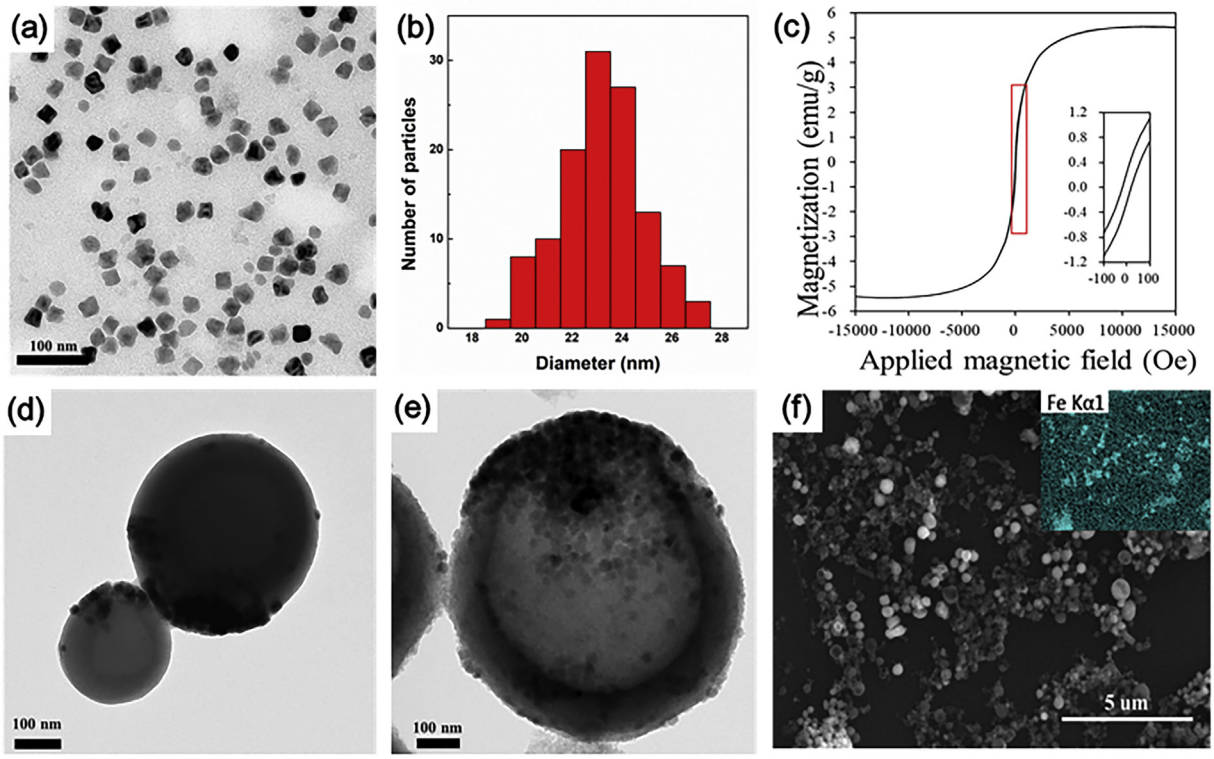

Fig. 2. (a) TEM image of IONP, (b) Histogram of the particles sizes of IONP, (c) magnetization curve of IONP, (d) TEM images of the IONP-containing droplets before coating silica, (e) TEM images of IONP-HMSs, and (f) SEM image of IONP-HMSs (inset: SEM-EDX elemental mapping for Fe).

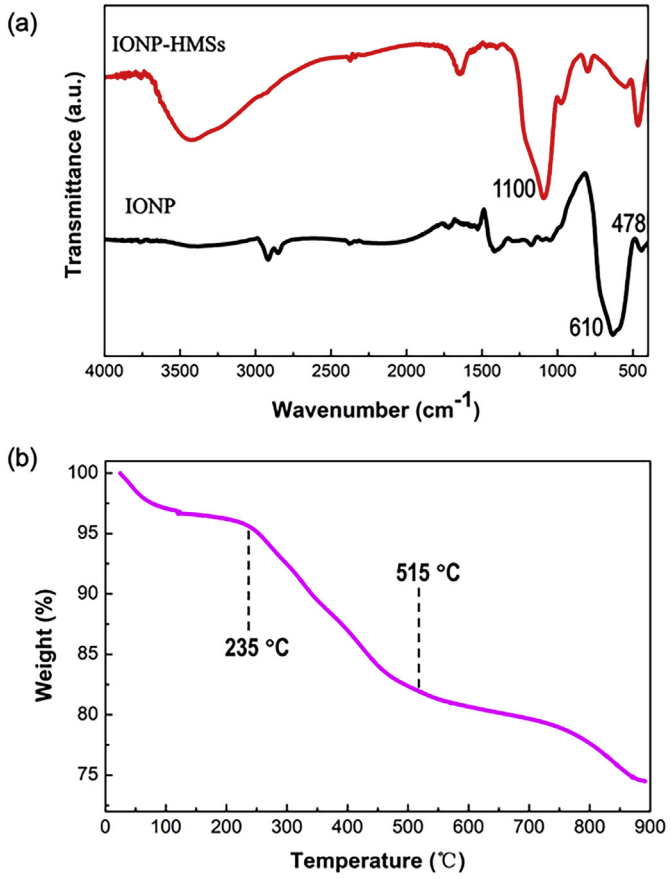

Fig. 3. (a) FTIR spectrum of IONP and IONP-HMSs, and (b) TGA curve of IONP-HMSs.

thermal decomposition method were modified with oleic acid [20,23], which acted as the capping agent for IONPs due to the strong affinity between the carboxylic group of oleic acid and surface atoms of iron oxide NPs [24]. Then the as-prepared IONPs dispersed in chloroform were transferred into the aqueous CTAB solution to form oil-in-water emulsions, in which the CTAB encapsulated IONP-containing spheres were used as templates to direct production of hollow mesoporous silica spheres. The surfactant CTAB serves as a phase transfer agent for oleic acid-capped IONP by coupling its alkyl chain to that of oleic acid through the hydrophobic van der Waals interactions, whilst the hydrophilic polar head group (N^+-$(CH_3)_3$) of CTAB facilitates the aqueous dispersion of IONPs with thermodynamically defined bilayer structures [25]. The hydrolyzation and condensation process of added TEOS resulted in the formation of amorphous silica on the surfaces of IONPs. Finally, the magnetic iron oxide nanoparticle-hollow mesoporous silica spheres (IONP-HMSs) were collected after refluxing to remove excess CTAB.

The transmission electron microscopy (TEM) image in Fig. 2(a) illustrated that the square-shape IONPs are monodisperse with the average size of 23.89 ± 1.6 nm (Fig. 2(b)). The magnetic properties of as-prepared IONPs were studied by measuring the hysteresis loop (MH curve). As shown in Fig. 2(c), the magnetization curve exhibiting magnetic remanence of 0.244 emu/g and coercivity of 18.8 Oe, respectively. Due to the magnetic remanence, the IONPs aggregated at one side of the CTAB encapsulated spheres, resulting in an IONP-capping morphology. The square-shape IONPs were assembled with CTAB encapsulation as shown in Fig. 2(d). After the hydrolyzation and condensation process of added TEOS, the mesoporous silica shells were coated onto the IONP-containing droplets. Finally, the TEM image of the IONP-HMSs with hollow interior cavity and mesoporous silica shell was shown in Fig. 2(e). The scanning electron microscopy (SEM) image of IONP-HMSs was presented in Fig. 2(f), and the EDX elemental mapping in the inset indicated the existence of Fe in IONP-HMSs. These results demonstrate the successful synthesis of IONP-HMSs based on an oil-in-water microemulsion system.

The Fourier transform infrared (FTIR) spectrum confirmed the formation of IONP-HMSs. As presented in Fig. 3(a), two characteristic strong absorption bands at 610 cm^{-1} and 478 cm^{-1} are corresponding to the Fe–O bond of IONPs [26,27]. The presented broad absorption band at 3300–3500 cm^{-1} is the indication of the existence of Si–O–H, and the active band located at around 1100 cm^{-1} is the stretching vibration of Si–O–Si, which identifies the presence of SiO_2 on the surface of IONPs [27,28]. Thermogravimetric analysis (TGA) was also carried out to verify the preparation of IONP-HMSs. The TGA curve in Fig. 3(b) shows that the total weight loss of IONP-HMSs was ~25.5%. The observed weight loss below 235 °C was attributed to the evaporation of residue organic solvent and water, while the main weight loss at 235–515 °C resulted from the dihydroxylation of silanol groups (Si–OH) of mesoporous silica shells. All these characterization results confirm the composition of prepared IONP-HMSs containing both magnetic nanoparticles and mesoporous silica shells.

The DOX molecules form strong π-π interactions with the surface of hollow silica sphere. The DOX loading on the surface of hollow silica sphere through π-π stacking mechanisms [29]. The hollow interior cavity offers IONP-HMSs sufficient capacity to carry drug molecules, while the mesopores shells can be used for drug transportation and pH-triggered drug release from the interior cavity [30]. Based on these characteristics, we explored the feasibility of IONP-HMSs as nanocarrier of anti-cancer drug. The DOX-adsorption capacity and DOX-loading efficiency of IONP-HMSs were determined by the UV–Vis absorbance at 480 nm [31]. Fig. 4(a) exhibited that both the DOX-adsorption capacity and loading efficiency of IONP-HMSs were enhanced with the increasing of DOX concentration from 100 μg/mL to 900 μg/mL. Finally, the DOX-adsorption capacity of IONP-HMSs reached 37.3%, while the DOX-loading efficiency achieved to 62.1%. Besides, the effect of pH values on the drug loading process was quantitatively investigated. As shown in Fig. 4(b), the DOX-adsorption capacity and DOX-loading efficiency of IONP-HMSs displayed an apparent increasing trend at pH = 7.4 compared with the case at pH = 5.0, owing to the improvement of interaction affinity between negatively-charged IONP-HMSs and positively-charged DOX molecules at high pH value [32]. All these results demonstrate that IONP-HMSs is a promising candidate for being utilized as nanocarrier in drug delivery system.

The cumulative DOX release profile of IONP-HMSs was recorded under acidic condition (pH = 5.0) and physiological-similar condition (pH = 7.4) at room temperature. As shown in Fig. 5, the amount of DOX-released from IONP-HMSs only achieved 12.7% after 6 h incubation and finally increased to 20.8% after 24 h at pH = 7.4. While in acidic condition with pH = 5.0, more than 30% DOX was rapidly released from DOX-loaded IONP-HMSs during the first 6 h and finally reached to 56.2% after two days of 48 h incubation. However, only 23.1% of DOX was released from IONP-HMSs at pH = 7.4 after 48 h. The results indicate that the drug release of IONP-HMSs could be triggered by acidic pH. This pH-triggered release property of DOX could be explained by the increased protonated carboxyl and amino groups on DOX in an acidic environment, which would weaken the binding force between DOX and nanoparticles [33–35]. The pH-triggered release strategy of DOX was desired in cancer therapy owing to the existence of cancer cells in an acidic environment.

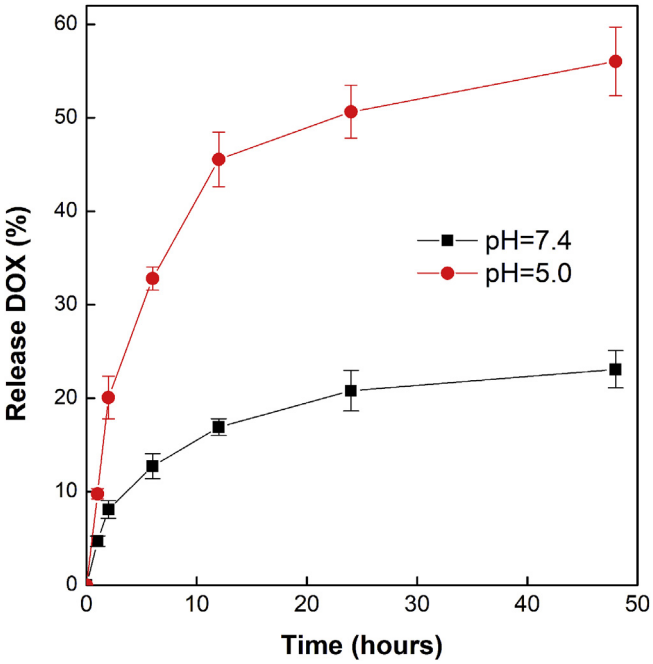

Fig. 5. Quantitative analyses of cumulative DOX-released from IONP-HMSs over time with different pH values at 7.4 and 5.0 (Notes: data are displayed as mean ± SD with n = 3).

The cell viability of IONP-HMSs to HeLa cells *in vitro* was

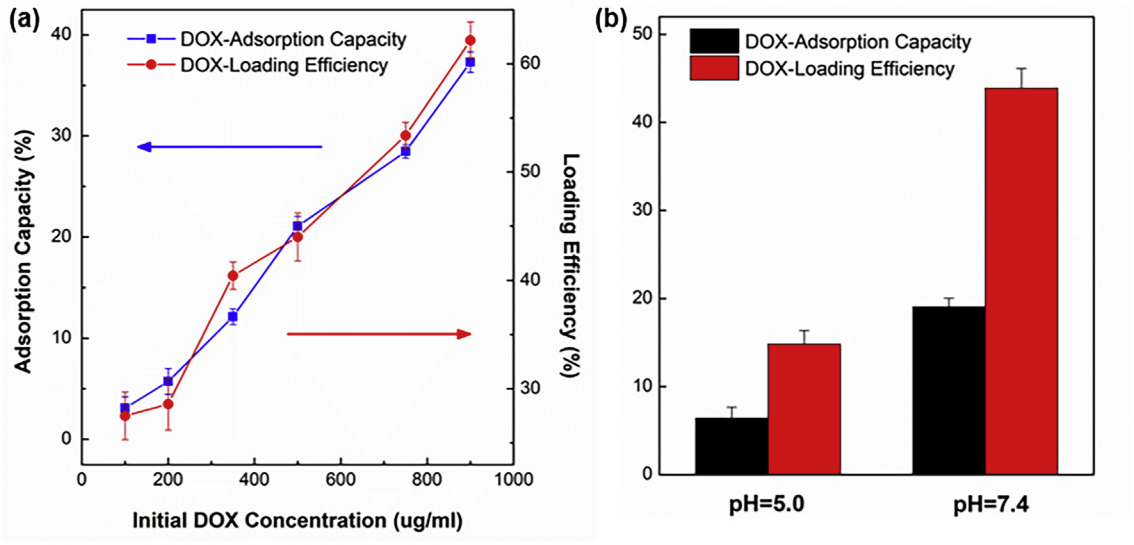

Fig. 4. (a) Quantitative analyses the effect of initial DOX concentration on DOX-adsorption capacity and DOX-loading efficiency of IONP-HMSs, and (b) Quantitative analyses the effect of pH values on DOX-adsorption capacity and DOX-loading efficiency of IONP-HMSs (Notes: data are displayed as mean ± SD with n = 3).

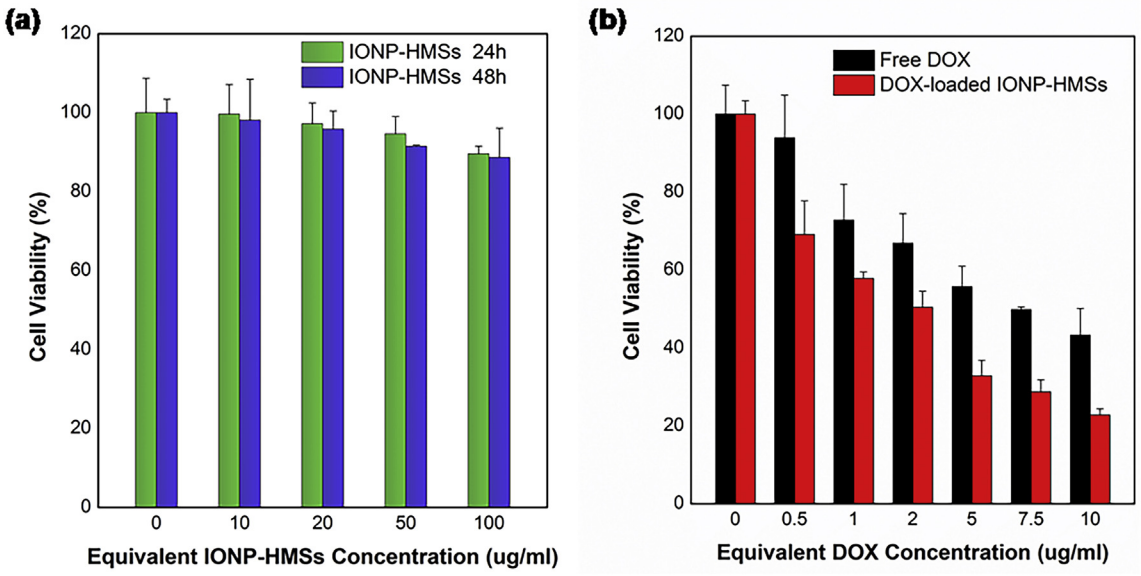

Fig. 6. (a) Cell viability of IONP-HMSs after 24 h and 48 h incubation, and (b) Cell viability profiles of free DOX and DOX-loaded IONP-HMSs after 24 h incubation (Notes: data are displayed as mean ± SD with n = 5).

investigated with an MTT assay as presented in Fig. 6(a), the IONP-HMSs showed the negligible cytotoxicity to HeLa cells after incubation of 24 h, and there were even more than 85% of cell viability after 48 h. These results indicate the biocompatibility of IONP-HMSs. Furthermore, the therapeutic efficacy of IONP-HMSs was studied through the comparison of the cell viability of DOX-loaded IONP-HMSs with the free DOX to HeLa cells with various concentrations (Fig. 6(b)). The cell viability of both DOX-loaded IONP-HMSs and free DOX were very close with lower concentration and then increased gradually with the increase of drug concentration. The HeLa cells treated by DOX-loaded IONP-HMS exhibited lower cell viability compared with that of free DOX under all the various concentration, revealing the enhancement of DOX therapeutic efficacy for HeLa cells via the conjugation with IONP-HMSs.

4. Conclusions

We have developed a facile method to fabricate the magnetic iron oxide nanoparticle-hollow mesoporous silica spheres (IONP-HMSs) via an oil-in-water microemulsion system, which contains the assembling process of square-shape IONPs and the later formation of mesoporous silica shell. This microemulsion-based method provides a simple way to produce hollow-structure nanocomposite without any complicated template-removing procedure. In our study, the magnetic property of IONPs has been investigated. The mesopores silica shell can be used for transportation and release of drug from the internal cavity due to the internal hollow cavity offering the ability to carry drug molecules. The as-prepared IONP-HMSs can act as the desired candidate of nanocarrier in drug delivery system as demonstrated by the investigation of DOX loading and pH-triggered release from IONP-HMSs in this paper. The cell viability test demonstrated the excellent biocompatibility of this IONP-HMSs and the enhanced therapeutic efficacy of this nanocarrier to HeLa cells.

In addition, since these IONP-HMSs can combine magnetic property of IONP and hollow mesoporous structure of silica spheres, in the future they could be applied to the development of magnetic drug delivery system that can be guided to the targeted domain by applying the magnetic field. The facile route for the synthesis of IONP-HMSs could be a promising platform for the future development of drug delivery and cancer therapy.

Ethics statement

Notes

- The authors declare they have no conflict of interests exits in the submission of this manuscript.
- Manuscript is approved by all authors for publication.
- I would like to declare on behalf of my co-authors that the work described was original research that has not been published previously, and not under consideration for publication elsewhere, in whole or in part.
- All the authors listed have approved the manuscript that is enclosed.

Acknowledgments

This research was supported by the Seed Funding Program for Basic Research, Seed Funding Program for Applied Research and Small Project Funding Program from University of Hong Kong, RGC-GRF grant (HKU 17204617), ITF Tier 3 funding (ITS-104/13, ITS-214/14), and University Grants Committee of HK (AoE/P-04/08).

References

[1] F. Xiong, S. Huang, N. Gu, Magnetic nanoparticles: recent developments in drug delivery system, Drug Dev. Ind. Pharm. 44 (2018) 697–706.
[2] D. Peer, J.M. Karp, S. Hong, O.C. Farokhzad, R. Margalit, R. Langer, Nanocarriers as an emerging platform for cancer therapy, Nat. Nanotechnol. 2 (2007) 751–760.
[3] D. Tarn, C.E. Ashley, M. Xue, E.C. Carnes, J.I. Zink, C.J. Brinker, Mesoporous silica nanoparticle nanocarriers: biofunctionality and biocompatibility, Acc. Chem. Res. 46 (2013) 792–801.
[4] S. Ganta, H. Devalapally, A. Shahiwala, M. Amiji, A review of stimuli-responsive nanocarriers for drug and gene delivery, J. Control. Release 126 (2008) 187–204.
[5] I. Roy, T.Y. Ohulchanskyy, H.E. Pudavar, E.J. Bergey, A.R. Oseroff, J. Morgan, T.J. Dougherty, P.N. Prasad, Ceramic-based nanoparticles entrapping water-insoluble photosensitizing anticancer drugs: a novel drug-carrier system for photodynamic therapy, J. Am. Chem. Soc. 125 (2003) 7860–7865.
[6] W.T. Al-Jamal, K. Kostarelos, Liposomes: from a clinically established drug delivery system to a nanoparticle platform for theranostic nanomedicine, Acc. Chem. Res. 44 (2011) 1094–1104.
[7] F. Wang, Y.C. Wang, S. Dou, M.H. Xiong, T.M. Sun, J. Wang, Doxorubicin-tethered responsive gold nanoparticles facilitate intracellular drug delivery for overcoming multidrug resistance in cancer cells, ACS Nano 5 (2011) 3679–3692.
[8] S. Laurent, D. Forge, M. Port, A. Roch, C. Robic, L. Vander Elst, R.N. Muller, Magnetic iron oxide nanoparticles: synthesis, stabilization, vectorization, physicochemical characterizations, and biological applications, Chem. Rev. 108 (2008) 2064–2110.
[9] C. Garcia, Y. Zhang, F. DiSalvo, U.J.A.C. Wiesner, Mesoporous aluminosilicate

materials with superparamagnetic γ-Fe2O3 particles embedded in the walls, Angew. Chem. Int. Ed. 115 (2003) 1564–1568.
[10] Q.J. He, M. Ma, C.Y. Wei, J.L. Shi, Mesoporous carbon@silicon-silica nanotheranostics for synchronous delivery of insoluble drugs and luminescence imaging, Biomaterials 33 (2012) 4392–4402.
[11] H.X. Wu, L.H. Tang, L. An, X. Wang, H.Q. Zhang, J.L. Shi, S.P. Yang, pH-responsive magnetic mesoporous silica nanospheres for magnetic resonance imaging and drug delivery, React. Funct. Polym. 72 (2012) 329–336.
[12] S. Liu, M.Y. Han, Silica-coated metal nanoparticles, Chem. Asian J. 5 (2010) 36–45.
[13] J. Kim, H.S. Kim, N. Lee, T. Kim, H. Kim, T. Yu, I.C. Song, W.K. Moon, T. Hyeon, Multifunctional uniform nanoparticles composed of a magnetite nanocrystal core and a mesoporous silica shell for magnetic resonance and fluorescence imaging and for drug delivery, Angew. Chem. Int. Ed. Engl. 47 (2008) 8438–8441.
[14] L. Zhang, S. Qiao, Y. Jin, H. Yang, S. Budihartono, F. Stahr, Z. Yan, X. Wang, Z. Hao, G.Q. Lu, Fabrication and size-selective bioseparation of magnetic silica nanospheres with highly ordered periodic mesostructure, Adv. Funct. Mater. 18 (2008) 3203–3212.
[15] K. Moller, T. Bein, Inclusion chemistry in periodic mesoporous hosts, Chem. Mater. 10 (1998) 2950–2963.
[16] B.G. Trewyn, J.A. Nieweg, Y. Zhao, V.S.-Y. Lin, Biocompatible mesoporous silica nanoparticles with different morphologies for animal cell membrane penetration, Chem. Commun. (Camb) 137 (2008) 23–29.
[17] Z. Feng, Y. Li, D. Niu, L. Li, W. Zhao, H. Chen, L. Li, J. Gao, M. Ruan, J. Shi, A facile route to hollow nanospheres of mesoporous silica with tunable size, Chem. Commun. (Camb) (2008) 2629–2631.
[18] Y. Chen, H. Chen, L. Guo, Q. He, F. Chen, J. Zhou, J. Feng, J.J.A.n. Shi, Hollow/rattle-type mesoporous nanostructures by a structural difference-based selective etching strategy, ACS Nano 4 (2009) 529–539.
[19] X.W. Lou, L.A. Archer, Z.J.A.M. Yang, Hollow micro-/nanostructures: synthesis and applications, Adv. Mater. 20 (2008) 3987–4019.
[20] C.R. Lin, R.K. Chiang, J.S. Wang, T.W. Sung, Magnetic properties of monodisperse iron oxide nanoparticles, J. Appl. Phys. 99 (2006) 08N710.
[21] R.K. Das, N. Kasoju, U.J.N.N. Bora, Biology, Medicine, Encapsulation of curcumin in alginate-chitosan-pluronic composite nanoparticles for delivery to cancer cells, Nanomed. Nanotechnol. Biol. Med. 6 (2010) 153–160.
[22] K.G.H. Desai, H.J. Park, Preparation and characterization of drug-loaded chitosan–tripolyphosphate microspheres by spray drying, Drug Dev. Res. 64 (2005) 114–128.
[23] Y. Teng, C. Jiang, A. Ruotolo, P.W.T. Pong, Amine-functionalized Fe2O3–SiO2 core–shell nanoparticles with tunable sizes, IEEE Trans. Nanotechnol. 17 (2018) 69–77.
[24] W.Y. William, J.C. Falkner, C.T. Yavuz, V.L.J.C.C. Colvin, Synthesis of monodisperse iron oxide nanocrystals by thermal decomposition of iron carboxylate salts, Chem. Commun. (Camb) (2004) 2306–2307.
[25] H. Fan, A. Wright, J. Gabaldon, A. Rodriguez, C.J. Brinker, Y.B. Jiang, Three-dimensionally ordered gold nanocrystal/silica superlattice thin films synthesized via sol–gel self-assembly, Adv. Funct. Mater. 16 (2006) 891–895.
[26] R. Sharma, S. Lamba, S. Annapoorni, Magnetic properties of polypyrrole-coated iron oxide nanoparticles, J. Phys. D Appl. Phys. 38 (2005) 3354–3359.
[27] M. Ma, Y. Zhang, W. Yu, H.Y. Shen, H.Q. Zhang, N. Gu, Preparation and characterization of magnetite nanoparticles coated by amino silane, Colloids Surf. A Physicochem. Eng. Asp. 212 (2003) 219–226.
[28] E.S. Lee, K.T. Oh, D. Kim, Y.S. Youn, Y.H. Bae, Tumor pH-responsive flower-like micelles of poly(L-lactic acid)-b-poly(ethylene glycol)-b-poly(L-histidine), J. Control. Release 123 (2007) 19–26.
[29] Y. Chen, H. Chen, M. Ma, F. Chen, L. Guo, L. Zhang, J. Shi, Double mesoporous silica shelled spherical/ellipsoidal nanostructures: synthesis and hydrophilic/hydrophobic anticancer drug delivery, J. Mater. Chem. 21 (2011) 5290–5298.
[30] E.S. Lee, K.T. Oh, D. Kim, Y.S. Youn, Y.H. Bae, Tumor pH-responsive flower-like micelles of poly (L-lactic acid)-b-poly (ethylene glycol)-b-poly (L-histidine), J. Control. Release 123 (2007) 19–26.
[31] J. Xu, L. Yang, Y. Han, Y. Wang, X. Zhou, Z. Gao, Y.Y. Song, P. Schmuki, Carbon-decorated TiO2 nanotube membranes: a renewable nanofilter for charge-selective enrichment of proteins, ACS Appl. Mater. Interfaces 8 (2016) 21997–22004.
[32] S. Wu, X. Zhao, Y. Li, Q. Du, J. Sun, Y. Wang, X. Wang, Y. Xia, Z. Wang, L. Xia, Adsorption properties of doxorubicin hydrochloride onto graphene oxide: equilibrium, kinetic and thermodynamic studies, Mater. 6 (2013) 2026–2042.
[33] L. Niu, L. Meng, Q.J.M.b. Lu, Folate-Conjugated PEG on single walled carbon nanotubes for targeting delivery of doxorubicin to cancer cells, Macromol. Biosci. 13 (2013) 735–744.
[34] Z. Liu, X. Sun, N. Nakayama-Ratchford, H. Dai, Supramolecular chemistry on water-soluble carbon nanotubes for drug loading and delivery, ACS Nano 1 (2007) 50–56.
[35] Z. Liu, A.C. Fan, K. Rakhra, S. Sherlock, A. Goodwin, X. Chen, Q. Yang, D.W. Felsher, H. Dai, Supramolecular stacking of doxorubicin on carbon nanotubes for in vivo cancer therapy, Angew. Chem. Int. Ed. Engl. 48 (2009) 7668–7672.